Bedrock Geology of the
Bethel Quadrangle, Maine

Bedrock geologic mapping by
J. Dykstra Eusden Jr., James J. Brady, Riley M. Eusden, Myles M. Felch,
Thorn K. Merrill, and Kurt A. Niiler

Digital cartography by
Amber T. H. Whittaker
Susan S. Tolman

Geologic editing by
Robert G. Marvinney
Amber T. H. Whittaker

Cartographic design by
Christian H. Halsted

Robert G. Marvinney
State Geologist

Funding for the preparation of this map was provided in part by the
U.S. Geological Survey STATEMAP Program, Cooperative Agreement Nos. G12AC20185 and G19AC00156.

Maine Geological Survey
Address: 93 State House Station, Augusta, Maine 04333
Telephone: 207-287-2801 **E-mail:** mgs@maine.gov
Home page: www.maine.gov/dacf/mgs/

Open-File No. 20-11
2020

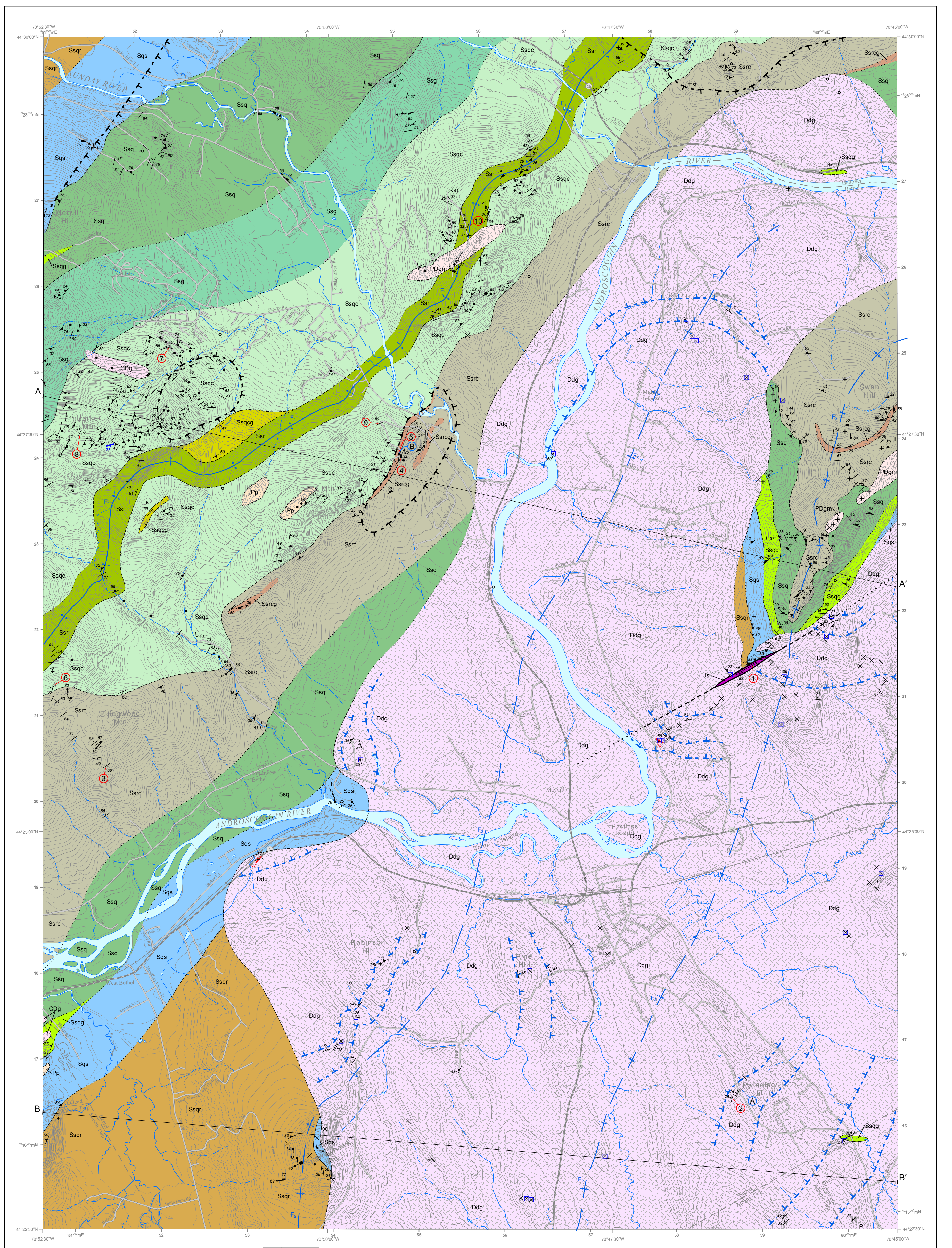

SOURCES OF GEOLOGIC INFORMATION

Field work by J. Dykstra Eusden and Riley Eusden, 2012; J. Dykstra Eusden, Myles Felch, Kurt Niiler, and Thorn Merrill, 2019.
James J. Brady, 1991 MS Thesis, University of Maine at Orono.

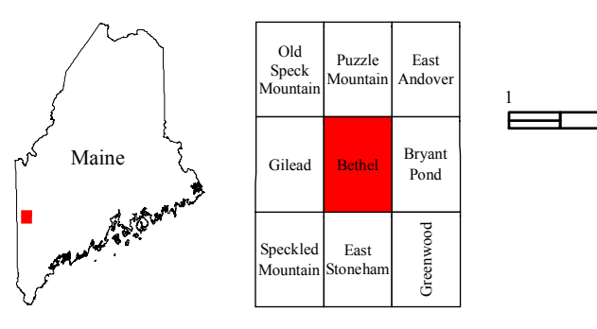

SCALE 1:24,000

CONTOUR INTERVAL 20 FEET

Approximate Mean Declination, 2019
15° W

Base map features from Maine Office of GIS - 1:24,000 USGS contour lines, E911 roads, 1:24,000 National Hydrography Dataset, USGS GNIS placenames and 1:24,000 political boundaries. Map projection Universal Transverse Mercator, North American Datum, 1927.

INTERPRETIVE CROSS SECTIONS

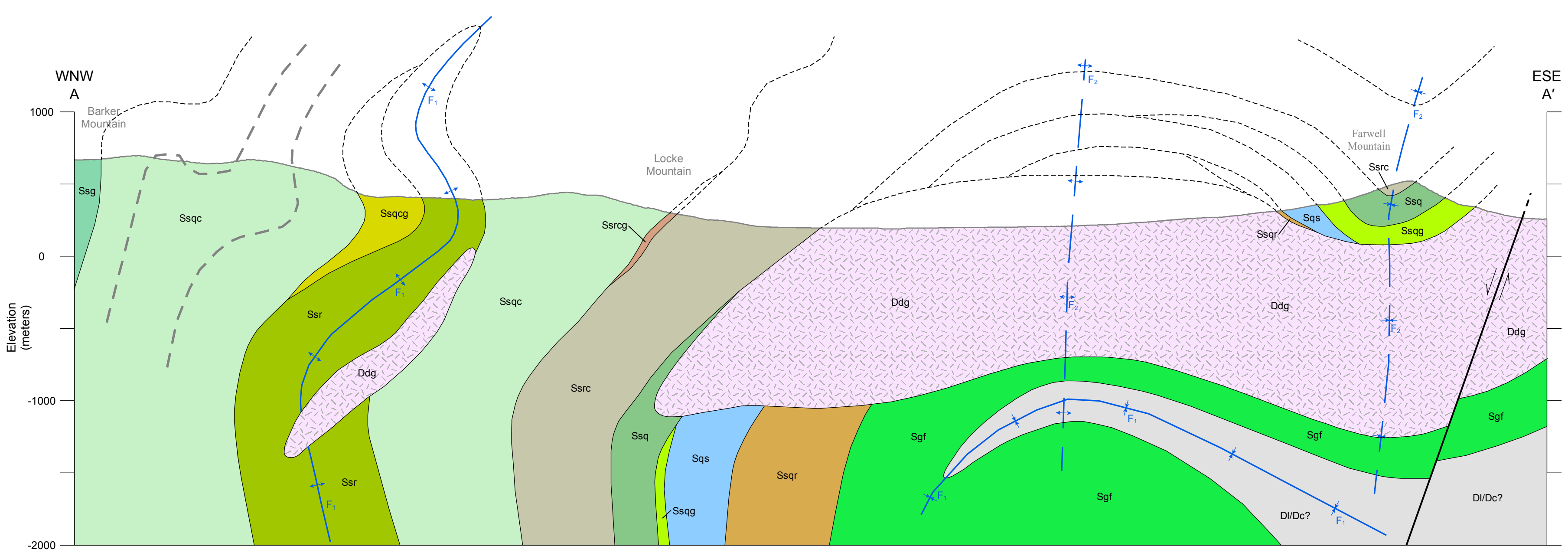

Contacts are dashed where projected above ground, solid where projected below ground.
Dashed gray lines represent intraformational structure.
No vertical exaggeration.

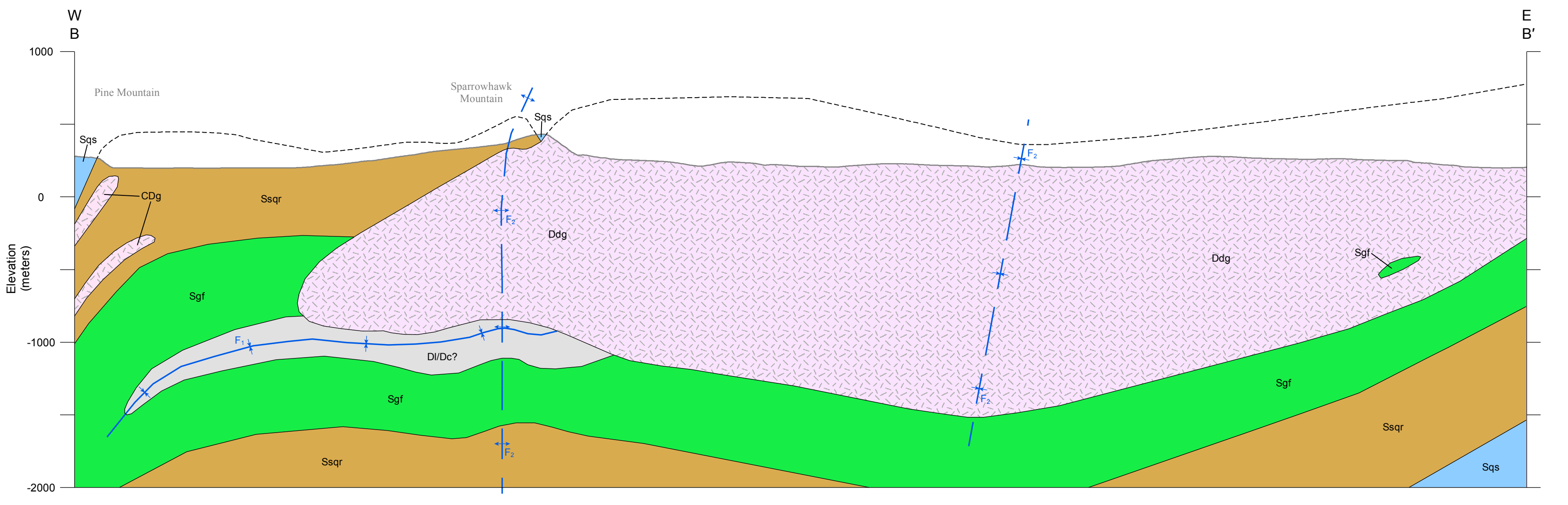

REFERENCES

Allmendinger, R., Cardozo, N., and Fisher, D., 2011, Structural Geology Algorithms: Vectors and Tensors. Cambridge: Cambridge University Press. doi:10.1017/CBO9780511920202

Bradley, D.C., and O'Sullivan, P., 2016, Detrital Zircon Geochronology of Pre- and Syncollisional Strata, Acadian Orogen, Maine Appalachians: Basin Research, v. 29, no. 5, p 571-590.

Bradley, D.C. and Tucker, R., 2002, Emsian Synorogenic Paleogeography of the Maine Appalachians: Journal of Geology, 110, 10/8/2013-483-492.

Bradley, D.C., Shea, E., Buchwaldt. R., Bowring, S., Benowitz, J., O'Sullivan, P.B., and Mccauley, A, 2016, Geochronology and tectonic context of lithium-cesium-tantalum pegmatites in the Appalachians: The Canadian Mineralogist, v. 54, p. 945-969.

Brady, J. J., 1991, The bedrock geology of the Bethel Maine area: M.S. thesis, University of Maine, Orono, Maine, 150 p.

Cardozo, N., and Allmendinger, R.W., 2013, Spherical projections with OSXStereonet: Computers & Geosciences, v. 51, p. 193 – 205, doi:10.1016/j.cageo.2012.07.021.

Eusden, J.D., 2010, The Presidential Range: Its Geologic and Tectonic History: Durand Press, Lyme, New Hampshire, 62 p and 1:20,000 map.

Eusden, J.D., Choe, S., Divan, E., Eusden, R., Watermulder, S., and Wheatcroft, A., 2018, Bedrock geology of the Gilead quadrangle, Maine: Maine Geological Survey, Open-File Map 18-12, scale 1:24,000. https://digitalmaine.com/mgs_maps/2069

Gibson, D., and Lux, D.R., 1989, Petrographic and geochemical variations within the Songo pluton, western Maine: in Tucker, RD., and Marvinney, R.G. (editors), Studies in Maine geology: Volume 4 - Igneous and metamorphic geology: Maine Geological Survey, p. 87-100.

Gibson, D., Osthoff, D., and Rerrick, C., 2017, Field relations, petrography and provenance of mafic dikes, western Maine: in Johnson, B. and Eusden, J.D. (editors), Guidebook for field trips in western Maine and northern New Hampshire: New England Intercollegiate Geological Conference, p. 273-286.

Hodge, D.S., Abbey, D.A., Harbin, M.A., Patterson, J.L., Ring, M.J., and Sweeney, J.F., 1982, Gravity Studies of Subsurface Mass Distributions of Granitic Rocks in Maine and New Hampshire: American Journal of Science, v. 282, p. 1289-1324.

Moench, R.H., Boudette, E.L., and Bothner, W.A., 1999, Tectonic lithofacies, geophysical, and mineral-resource appraisal maps of the Sherbrooke-Lewiston area, Maine, New Hampshire, and Vermont, United States, and Quebec, Canada: U.S. Geological Survey, Miscellaneous Investigations Series Map, 1-1898-E, 114 p, 3 sheets.

Nielson, D. L., Clark, R. G., Lyons, J. B., England, E. J., and Borns, D. H., 1976, Gravity Models and Mode of Emplacement of the New Hampshire Plutonic Series: in Lyons, P. C., and Brownlow, H. H. (editors), Studies of New England geology: Geological Society of America Memoir 146, p. 301-318.

Solar, G.S., and Tomascak, P.B., 2016, The Migmatite-Granite Complex of southern Maine: Its structure, petrology, geochemistry, geochronology, and relation to the Sebago Pluton: in Berry, H.N., IV, and West. D.P., Jr. (editors), Guidebook for field trips along the Maine coast from Maquoit Bay to Muscongus Bay: New England Intercollegiate Geological Conference, p. 19-42.

Solar, G.S., Tomascak, P.B., and Brown, M., 2017, Relations between deformation, metamorphism, melting and pluton emplacement at the migmatite front: in Johnson, B., and Eusden, J.D. (editors), Guidebook for field trips in western Maine and northern New Hampshire: New England Intercollegiate Geological Conference, p. 217-246.

Thompson, W.B., 2008, Surficial geology of the Bethel quadrangle, Maine: Maine Geological Survey, Open-File Map 08-79, scale 1:24,000. https://digitalmaine.com/mgs_maps/2032

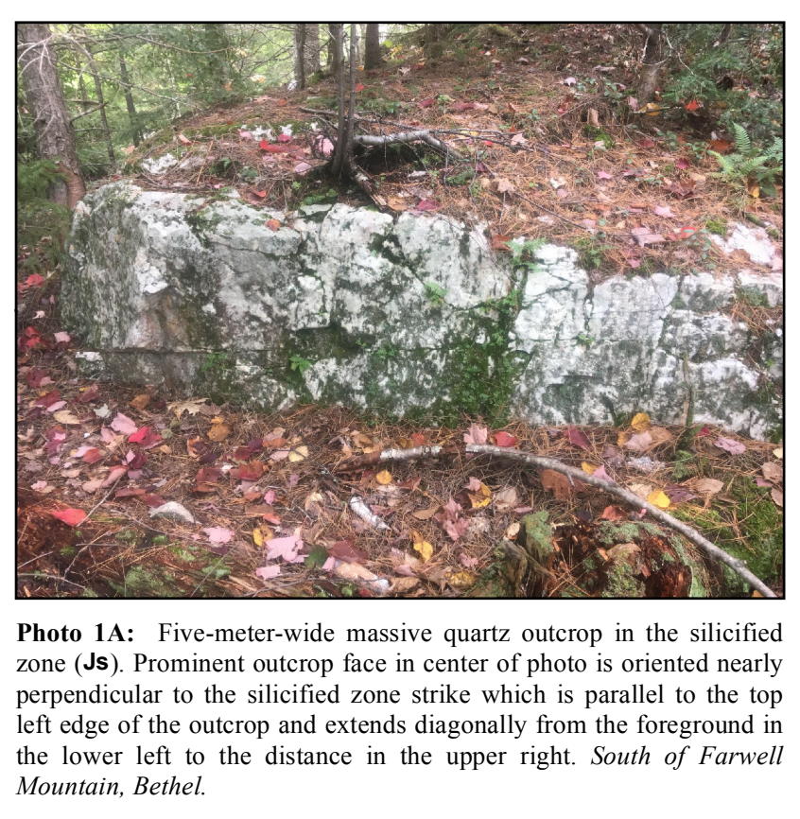

Photo 1A: Five-meter-wide massive quartz outcrop in the silicified zone (**Js**). Prominent outcrop face in center of photo is oriented nearly perpendicular to the silicified zone strike which is parallel to the top left edge of the outcrop and extends diagonally from the foreground in the lower left to the distance in the upper right. *South of Farwell Mountain, Bethel.*

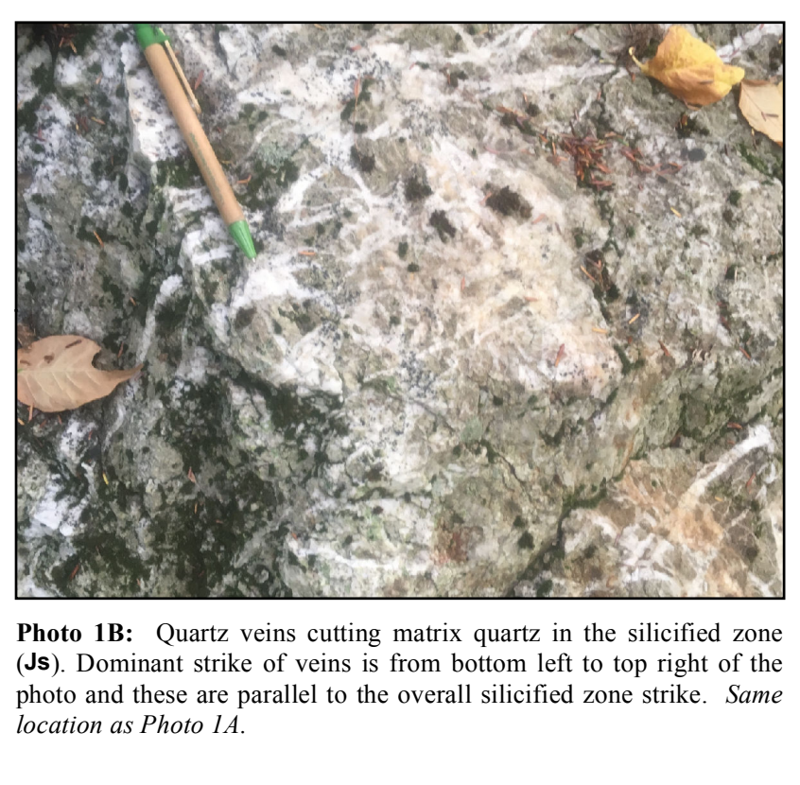

Photo 1B: Quartz veins cutting matrix quartz in the silicified zone (**Js**). Dominant strike of veins is from bottom left to top right of the photo and these are parallel to the overall silicified zone strike. *Same location as Photo 1A.*

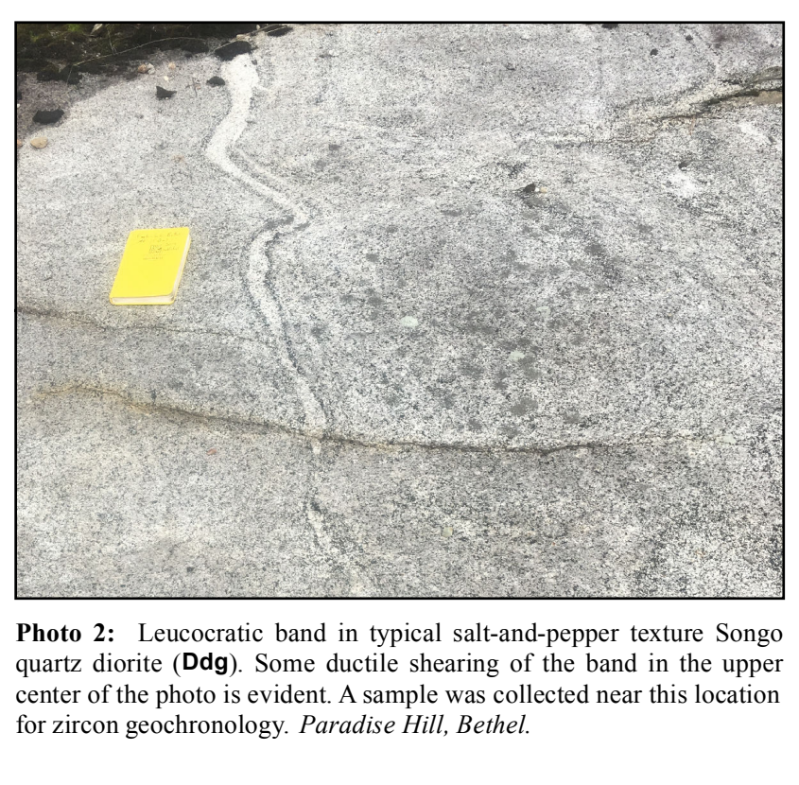

Photo 2: Leucocratic band in typical salt-and-pepper texture Songo quartz diorite (**Ddg**). Some ductile shearing of the band in the upper center of the photo is evident. A sample was collected near this location for zircon geochronology. *Paradise Hill, Bethel.*

Photo 3: Red-brown, deeply rusty weathering, sulfidic, thinly interbedded (1-2 cm) schist and quartzite. From map unit **Ssrc**. *1700 feet south of the top of Ellingwood Mountain.*

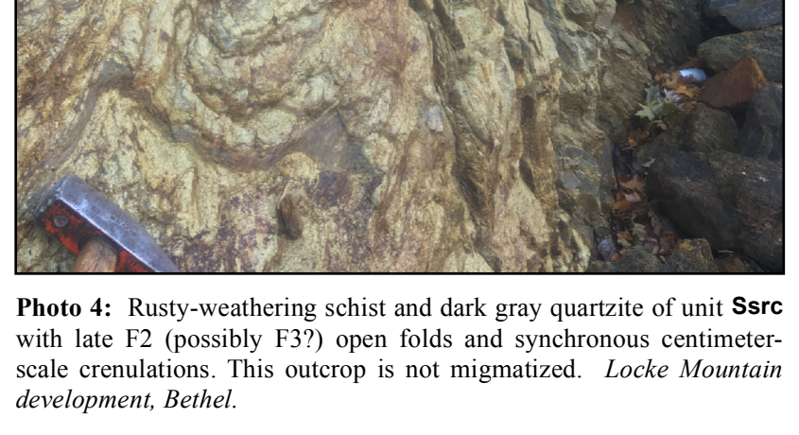

Photo 4: Rusty-weathering schist and dark gray quartzite of unit **Ssrc** with late F2 (possibly F3?) open folds and synchronous centimeter-scale crenulations. This outcrop is not migmatized. *Locke Mountain development, Bethel.*

Photo 5: Dark gray biotite granofels layers with greenish-pink calc-silicate layers in unit **Ssrcg**. A sample was collected here for detrital zircon geochronology (Location **B**). This outcrop is not migmatized. *Locke Mountain development, Bethel, near **Photo 4**.*

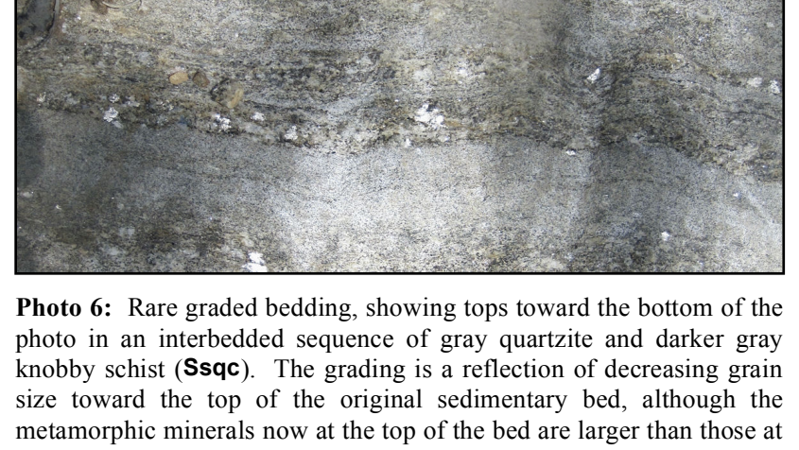

Photo 6: Rare graded bedding, showing tops toward the bottom of the photo in an interbedded sequence of gray quartzite and darker gray knobby schist (**Ssqc**). The grading is a reflection of decreasing grain size toward the top of the original sedimentary bed, although the metamorphic minerals now at the top of the bed are larger than those at the base. *Northwest of Ellingwood Mountain, at the west edge of the quadrangle.*

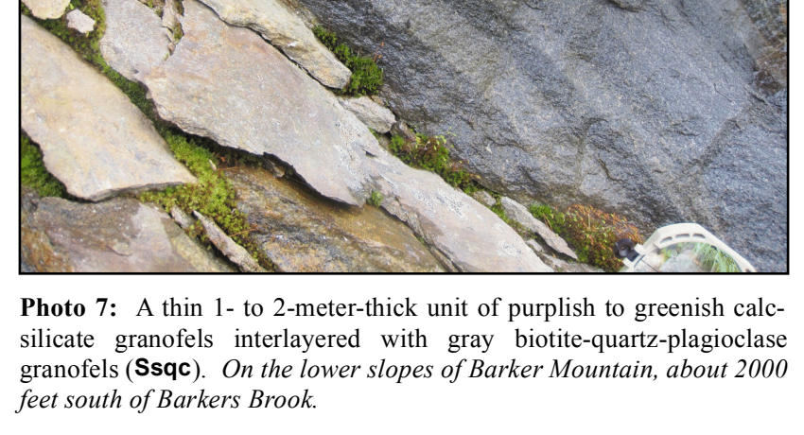

Photo 7: A thin 1- to 2-meter-thick unit of purplish to greenish calc-silicate granofels interlayered with gray biotite-quartz-plagioclase granofels (**Ssqc**). *On the lower slopes of Barker Mountain, about 2000 feet south of Barkers Brook.*

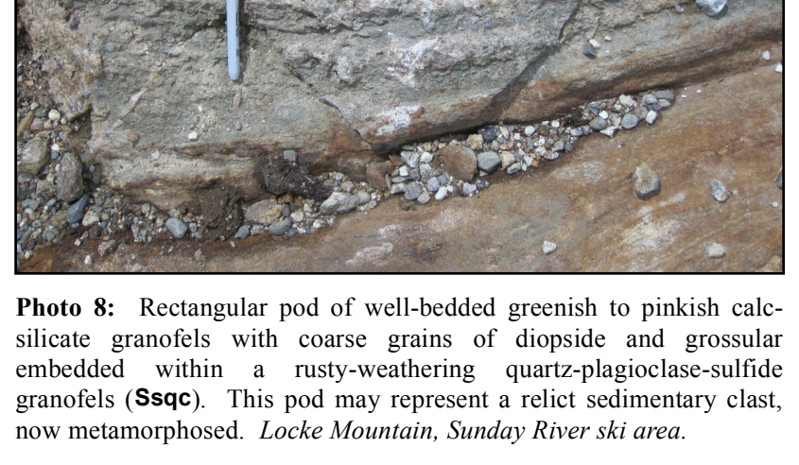

Photo 8: Rectangular pod of well-bedded greenish to pinkish calc-silicate granofels with coarse grains of diopside and grossular embedded within a rusty-weathering quartz-plagioclase-sulfide granofels (**Ssqc**). This pod may represent a relict sedimentary clast, now metamorphosed. *Locke Mountain, Sunday River ski area.*

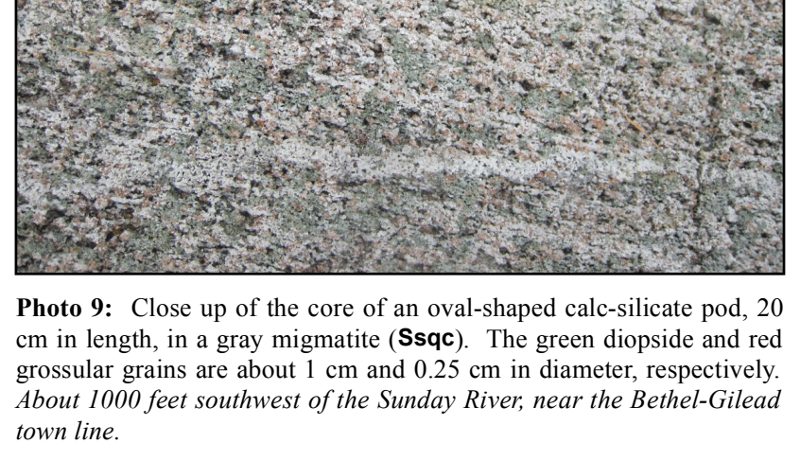

Photo 9: Close up of the core of an oval-shaped calc-silicate pod, 20 cm in length, in a gray migmatite (**Ssqc**). The green diopside and red grossular grains are about 1 cm and 0.25 cm in diameter, respectively. *About 1000 feet southwest of the Sunday River, near the Bethel-Gilead town line.*

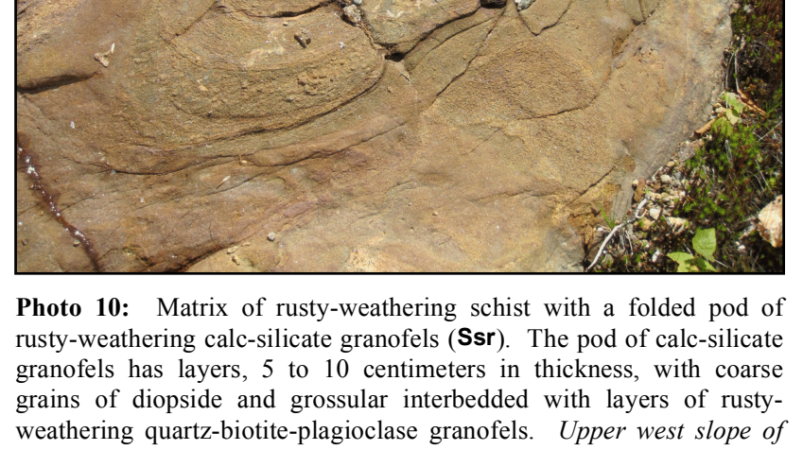

Photo 10: Matrix of rusty-weathering schist with a folded pod of rusty-weathering calc-silicate granofels (**Ssr**). The pod of calc-silicate granofels has layers, 5 to 10 centimeters in thickness, with coarse grains of diopside and grossular interbedded with layers of rusty-weathering quartz-biotite-plagioclase granofels. *Upper west slope of Mount Will.*

EXPLANATION OF UNITS

INTRUSIVE ROCKS

Jurassic(?) [J]

Js **Silicified zone.** Region of nearly pure white quartz with occasional rusty-weathering areas and numerous white quartz veins cutting the quartz matrix that are sometimes vuggy with well formed small (centimenter-sized) quartz crystals (**Photos 1A, 1B**). The zone dips steeply to the northwest, based on attitude of quartz veins, and varies from 1 meter (m) to 20 m in width. The outcrops of this unit weather positively as ridges and often form lineaments seen on the lidar hillshade image. Interpreted to be a late brittle fault (probable normal movement, north side down?).

Early Permian(?) [P]

Pp **Pegmatite.** Very coarse to coarse-grained white pegmatite. Minerals include quartz, feldspar, muscovite, ± biotite and ± tourmaline. Observed mineral grain size is typically less than 5 centimeters (cm) (2 inches [in]) in length and width, with extreme cases up to 30 cm (12 in) in length. Sizes of the distinct mineral types varied at each pegmatite outcrop. In most instances mappable pegmatite bodies form tops of small hills in the region resting above metasedimentary rocks. There are also numerous pegmatite intrusions at the majority of metasedimentary migmatite outcrops that are too small to show on the map.

Permian-Devonian(?) [PD]

PDgm **Muscovite-biotite granite and pegmatite, undifferentiated.** Medium-grained to fine-grained granite, locally containing garnet ± tourmaline. Pegmatite of the same mineralogy occurs with the granite, in various proportions. This granite and pegmatite unit occurs in several mostly small, mappable plutons. Dikes and sills of the same granite and pegmatite are also present throughout the migmatite regions. This granite may be related to granites of the Sebago pluton in southern Maine. Aside from the presence of pegmatites, similar to **CDgm** but differentiated in age by geochronology done for Gilead quadrangle in the vicinity of Wheeler Mine (Eusden and others, 2018).

Carboniferous-Devonian [CD]

CDg **Muscovite-biotite granite.** Medium-grained equigranular granite. Mottled appearance due to the combination of minerals including quartz, potassium and plagioclase feldspars, muscovite, biotite, and accessory minerals. The plutons were injected as sills mostly following strike of the metasedimentary units, and present as oblong ellipses in map view. Similar to **PDgm** but differentiated in age by geochronology done for Gilead quadrangle in the vicinity of Wheeler Mine (Eusden and others, 2018).

Devonian(?) [D]

Ddg **Quartz diorite, granodiorite, and rare pink granite, undifferentiated, of the Songo pluton.** Medium-grained to coarse-grained, equigranular, "salt-and-pepper" quartz diorite and/or granodiorite (**Photo 2**). Rare porphyritic zones are found with plagioclase phenocrysts up to 2 cm in size. Mineralogy is plagioclase feldspar, quartz, biotite, ± sphene, ± amphibole, ± potassium feldspar. This pluton makes up the majority of the eastern half of the quadrangle and represents the northern and western part of the Songo pluton. Igneous layering on the cm scale is rarely observed and defined by alternating layers of biotite-rich, darker quartz diorite or granodiorite and biotite-poor, lighter quartz diorite and granodiorite. In places the pluton exhibits a biotite foliation that varies in intensity, but in other areas the pluton is unfoliated. Shearing is sporadically observed and defined by ductile shear bands of igneous layering. Metasedimentary xenoliths, in particular biotite granofels and black biotite schist, are found in numerous regions within the unit and may have measured bedding or foliation, designated by an **x** (see **Explanation of Symbols**). Two outcrops of coarse-grained pink biotite granite were observed within this unit but were not large enough to differentiate. These outcrops are marked with a **p**.

STRATIFIED ROCKS

Note: References to named formations are those described by Moench and Boudette, 1987.

Devonian(?) [D]

Dl/Dc? **Littleton/Carrabassett Formation.** [Shown only in cross section, not shown on the map.] The following description is from Eusden (2010). Gray schist and quartzite often exhibiting graded bedding. Calc-silicate pods rare or absent. Centimeter-scale garnet coticule layers are infrequently found. This unit is not exposed at the surface in the Bethel quadrangle, but is inferred to lie stratigraphically above the biotite granofels unit (**Sgf**; possibly correlated with the Madrid Formation) and occupy the core of the recumbent syncline interpreted at depth. This relationship is observed in the adjacent Presidential Range of New Hampshire (Eusden, 2010).

Silurian(?) [S]

Sgf **Biotite granofels.** [Shown only in cross section, not shown on the map.] The following description is from Eusden and others (2018). Dark gray plagioclase-quartz-biotite granofels interlayered with rare purplish-gray to green calc-silicate granofels and gray schist. Layers of gray mica schist in places. (Possibly correlates with the Madrid Formation.) This unit is not exposed at the surface in the Bethel quadrangle, but is inferred to be present in the subsurface stratigraphically above the rusty-weathering schist and quartzite unit (**Ssqr**; possibly correlated with the Smalls Falls Formation) based on relationships observed to the west in the adjacent Gilead quadrangle (Eusden and others, 2018).

Ssqr **Moderately rusty weathering schist and quartzite with rare sections of deeply rusty weathering schist and quartzite.** Red-brown rusty-weathering, locally pyrrhotitic mica schist, interbedded with gray quartzite. Calc-silicate pods are rare or absent. (Possibly correlates with the Smalls Falls Formation.)

Sqs **Quartzite with gray schist, undifferentiated.** Light gray quartzite, in beds of variable thickness; well bedded and poorly graded. Contains thin interbeds of gray schist, 1 to 5 cm in thickness. Some sections have abundant calc-silicate pods, while in other sections they are rare or absent. (Possibly correlates with the Perry Mountain Formation.)

Ssq **Interbedded gray schist and quartzite, undifferentiated.** Heterogeneous unit consisting of gray mica schist with thin (1-5 cm) quartzite interbeds. Subordinate rusty-weathering schist, biotite granofels, and calc-silicate granofels. Calc-silicate pods are common to rare in the unit. (Possibly part of the Rangeley Formation.)

Ssqg **Biotite granofels.** Medium-grained, granoblastic quartz-plagioclase-biotite granofels, with rare calc-silicate granofels layers and minor gray schist.

Ssg **Gray schist.** Gray mica schist with rare interbedded thin (1-5 cm) quartzite and regions of rusty-weathering schist. Calc-silicate pods rare or absent. **Ssg** is stratigraphically equivalent to **Ssrc**. (Possibly part of the Rangeley Formation.)

Ssrc **Moderately rusty weathering to gray schist and quartzite with sections of deeply rusty weathering schist and quartzite.** Red-brown rusty-weathering mica schist with thin (1-5 cm) quartzite interbeds (**Photos 3** and **4**). Minor discontinuous layers 1-3 meters thick of quartz-plagioclase-biotite granofels and calc-silicate granofels, some mappable (**Ssrcg**). Some calc-silicate layers contain calcite. Calc-silicate pods rare or absent. **Ssrc** is stratigraphically equivalent to **Ssg**. (Possibly equivalent to part of the Rangeley or the Smalls Falls Formation.)

Ssrcg **Biotite granofels.** Medium-grained, granoblastic quartz-plagioclase-biotite granofels, with rare calc-silicate granofels layers and minor gray schist (**Photo 5**).

Ssqc **Gray schist and quartzite with calc-silicate pods.** Heterogeneous unit of variably interbedded gray schist and quartzite (1-5 cm; **Photo 6**), with rare, discontinous layers 1-3 meters in thickness of quartz-plagioclase-biotite granofels (**Photo 7**), and blocks of bedded, slightly rusty weathering granofels in migmatite (**Photo 8**). Calc-silicate pods are common throughout the unit (**Photo 9**). (Possibly part of the Rangeley

Ssqcg **Biotite granofels.** Medium-grained, granoblastic quartz-plagioclase-biotite granofels, with rare calc-silicate granofels layers and minor gray schist.

Ssr **Moderately rusty weathering schist.** Red-brown moderately rusty weathering mica schist with rare interbedded quartzite, and minor, discontinuous layers 1-3 meters thick of quartz-plagioclase-biotite granofels. Calc-silicate pods are common throughout the unit (**Photo 10**). (Possibly part of the Rangeley Formation.)

EXPLANATION OF LINES

Contact between rock units, of stratigraphic or intrusive origin
(well located, approximately located, poorly located).

High-angle fault, interpreted from truncation of map units, disruption of stratigraphic sequence, or rock deformation.
(well located, approximately located, poorly located).

Boundary of migmatite area. May be a sharp or gradational boundary. Hachures point toward migmatitic rocks.

Schematic representation of foliation orientations within the Songo pluton (**Ddg**). Hachures point down dip.

F_1 F_1 F_2 F_2

Trace of the axial surface of a regional anticline or syncline that formed early in the deformational sequence (F_1), or local antiforms and synforms that formed late in the deformational sequence (F_2).
Locations interpreted from map pattern of curved unit contacts.

EXPLANATION OF SYMBOLS

Note: Structural symbols are drawn parallel to strike or trend of measured structural feature. Barb or tick indicates direction of dip, if known. Annotation gives dip or plunge angle, if known. For most planar features, symbol is centered at observation point; for joints, observation point is at end of strike line opposite dip tick. For linear features, tail of symbol is at observation point. Multiple measurements at a site are represented by combined symbols. Symbols on the map are graphical representations of information stored in a bedrock database at the Maine Geological Survey. The database contains additional information that is not displayed on this map.

- • Outcrop of mapped unit.
- ○ Float, presumed to represent underlying bedrock.
- × Outcrop of non-foliated plutonic rock. **p** = pink granite.
- + Outcrop of pegmatite.
- □ 20 Pink pegmatite (occurrence, inclined vein). Coarse-grained pegmatite exclusively found within, and likely co-magmatic with, the Songo pluton (**Ddg**). Mineralogy: large (up to 10 cm, but commonly 2-4 cm) pink potassium feldspar, quartz, and biotite. Occurs as cm-scale irregular lenses and blobs and also as discrete, narrow (2-10 cm wide) veins cutting the Songo quartz diorite or granodiorite.
- 20 Quartz vein (inclined) in the silicified zone (**Js**).
- 20 Basalt dike, presumably of Jurassic age (inclined).
- 20 Sill of muscovite-biotite granite (inclined).
- 20 20 20 Bedding (inclined, top direction indicated; inclined, bedding overturned; inclined, top direction unknown; vertical, top direction unknown). **x** = xenolith.
- 20 Foliation in metamorphic rock (inclined). **x** = xenolith.
- 20 Foliation in igneous rock (inclined).
- 20 20 20 Structural elements of folds which deform bedding and schistosity, and so are younger than the schistosity (fold hinge, plunging, with unknown asymmetry; fold hinge, plunging, with right-handed asymmetry;axial plane, inclined; axial plane, vertical).
- 20 Joint (inclined, vertical).
- ① Photo location.
- Ⓐ Geochronology sample location (see **Table 1**).

TABLE 1: GEOCHRONOLOGY

Location	Unit	Mineral	Method	Age±2σ (Ma)	Reference
A	**Ddg**	Zircon	U-Pb	**360.7 ± 2.2**	Eusden, this study
B	**Ssrcg**	Detrital zircon	U-Pb	**430.3 ± 1.6**	Eusden, this study

Locations are shown on the map by a letter in a blue circle.
Detrital zircon ages are maximum depositional ages; zircon ages are crystallization ages.

PLOTS OF GEOCHRONOLOGICAL DATA

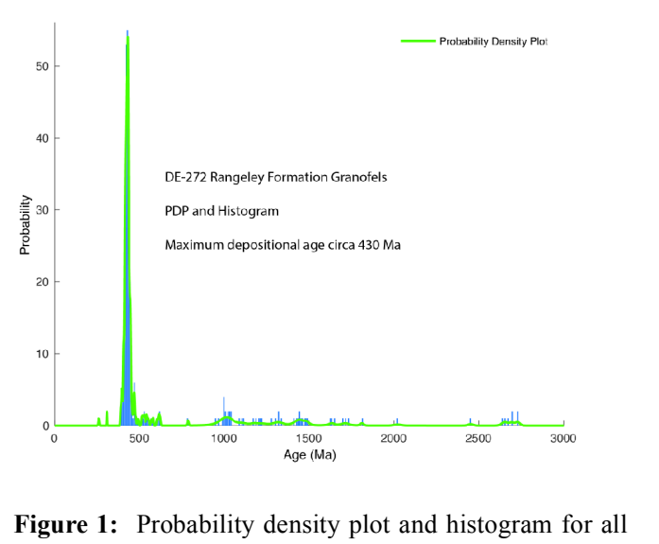

Figure 1: Probability density plot and histogram for all detrital zircons (n = 281) from unit **Ssrcg**.

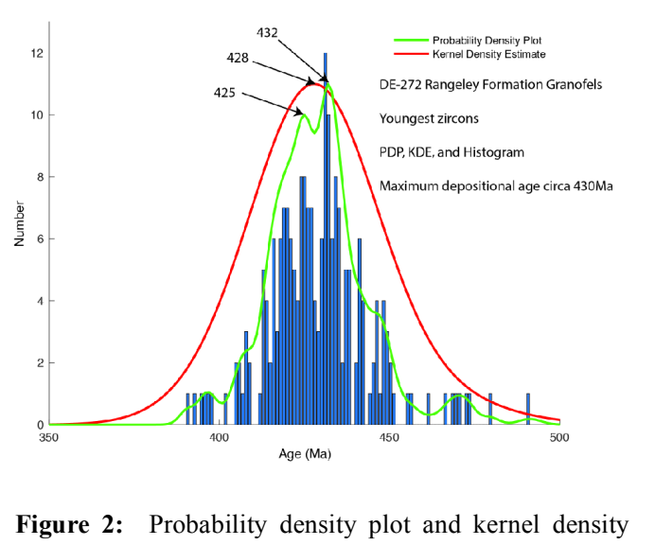

Figure 2: Probability density plot and kernel density estimate for the youngest detrital zircons (n = 214) from unit **Ssrcg**.

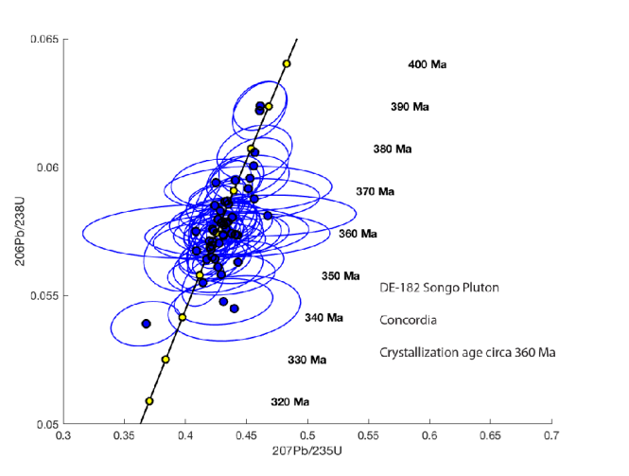

Figure 3: Concordia age diagram for a zircon sample (n=49) from the Songo pluton (**Ddg**).

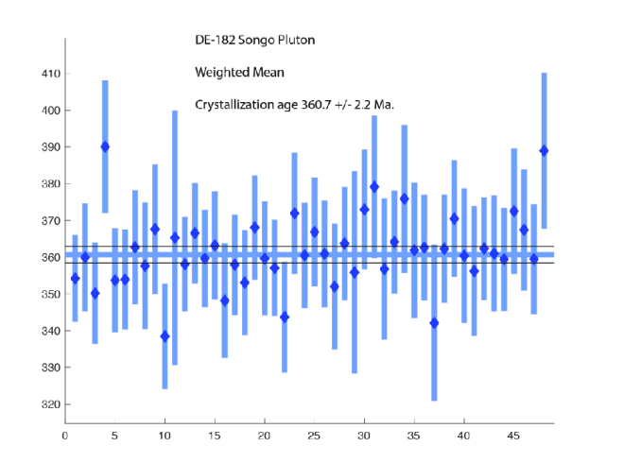

Figure 4: Weighed mean diagram for a zircon sample (n=49) from the Songo pluton (**Ddg**).

PLOTS OF STRUCTURAL DATA

The orientations of planar and linear features of the bedrock structure have been measured at various locations in the field. Oriented symbols are plotted on the map where each feature was measured. In order to compare orientations of features from various locations across the map, their orientations can be plotted together on a diagram designed for that purpose. A stereogram is a circular plot on which three-dimensional orientations of lines or planes can be shown. The orientation of a linear feature is represented by a point on the diagram and the orientation of a planar feature by a straight or curved line on the diagram. The strike or plunge azimuth can be read from the outer edge of the plot in relation to north, east, south, and west (N, E, S, and W) as you would read a compass. The inclination from horizontal is related to distance toward the center of the plot; points that plot at the edge of the circle have zero plunge and those at the center plunge 90 degrees. Planes represented by curved lines dip in the direction of the curve, the greater the curve the shallower the dip; planes represented by straight lines are vertical. For convenience, a plane may be represented by plotting its pole (a line perpendicular to the plane), greatly simplifying the plot if there is a large number of measurements. The mathematical construction shown in **Figures 5 - 7** is termed a cylindrical best fit or π diagram and assumes the folds in the region are shaped like a half tube or half cylinder. The Bingham axial distribution is to determine the trend and plunge of the fold axes. The routine works by calculating the orientation tensor from the direction cosines of the individual measurements and then calculating the eigenvalues and eigenvectors to get the principal axes of the tensor. The first axis corresponds to the greatest concentration of points, the second to the intermediate and the third to the smallest concentration; the third axis is usually interpreted as the cylindrical fold axis (Allmendinger and others, 2011; Cardozo and Allmendinger, 2013).

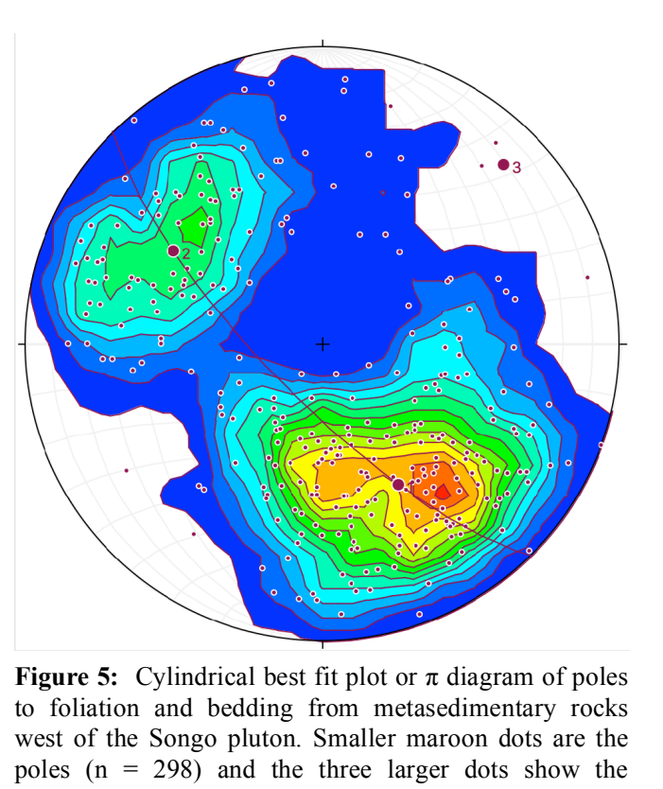

Figure 5: Cylindrical best fit plot or π diagram of poles to foliation and bedding from metasedimentary rocks west of the Songo pluton. Smaller maroon dots are the poles (n = 298) and the three larger dots show the eigenvectors for the cylindrical best fit. The Eigenvector labeled 3 records the trend and plunge of the calculated late fold axis which in this case is 045°, 15°.

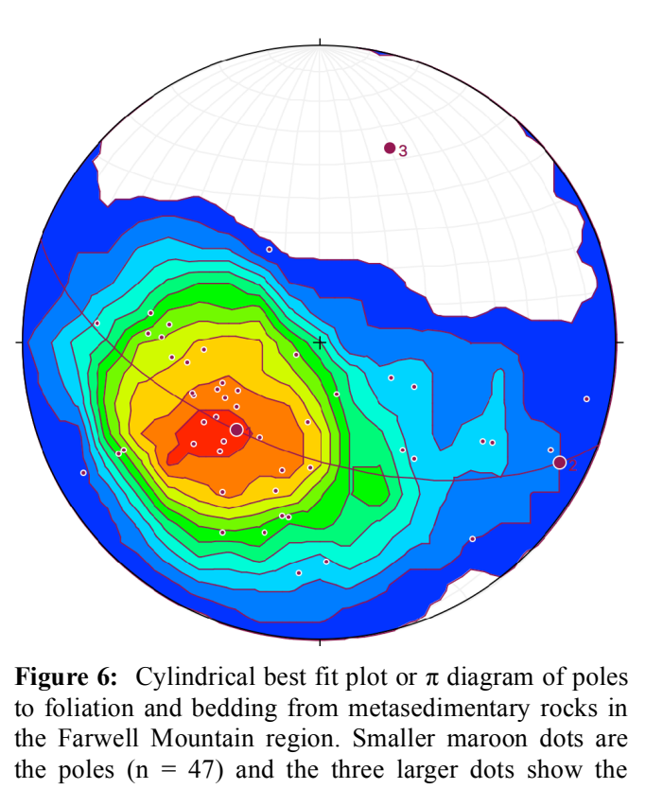

Figure 6: Cylindrical best fit plot or π diagram of poles to foliation and bedding from metasedimentary rocks in the Farwell Mountain region. Smaller maroon dots are the poles (n = 47) and the three larger dots show the eigenvectors for the cylindrical best fit. The Eigenvector labeled 3 records the trend and plunge of the calculated late fold axis which in this case is 020°, 31°.

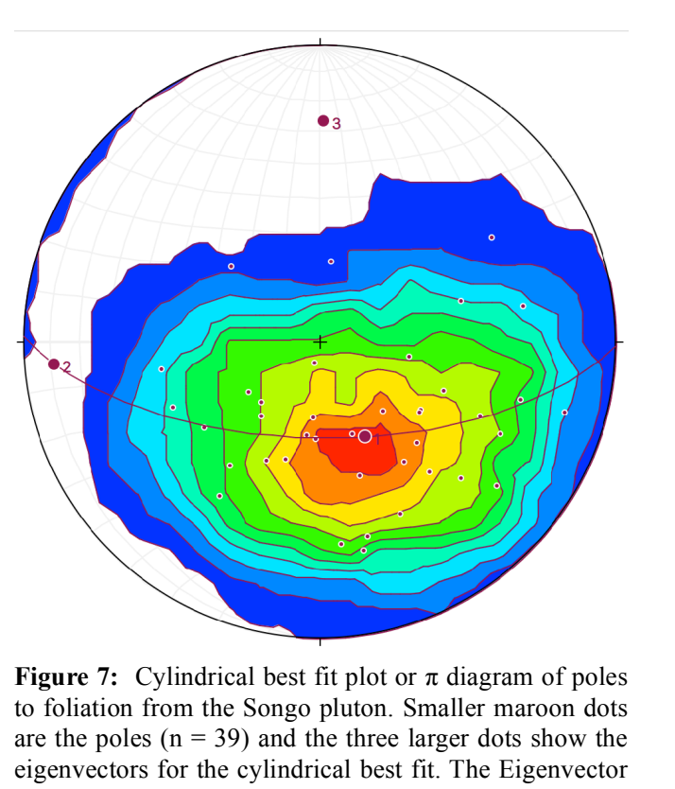

Figure 7: Cylindrical best fit plot or π diagram of poles to foliation from the Songo pluton. Smaller maroon dots are the poles (n = 39) and the three larger dots show the eigenvectors for the cylindrical best fit. The Eigenvector labeled 3 records the trend and plunge of the calculated late fold axis which in this case is 009°, 27°.

BEDROCK GEOLOGY OF THE BETHEL QUADRANGLE

INTRODUCTION TO THE MAP

The bedrock geologic map of the Bethel, Maine, quadrangle shows a geologist's interpretation of the distribution of the rock types in the region based upon data collected in the field. The challenging part of this process is that most of the bedrock, up to 80% or more, is covered by vegetation, soil, and/or glacial deposits, making the locational choices of boundaries between rocks at times very difficult to determine. In the Bethel quadrangle there were regions with excellent outcrop density, such as the Sunday River ski trails, and areas with poor outcrop, such as spruce-dominated forests above 3,000 feet and lower elevation valley and swampy regions with thick glacial cover. The field data is represented by various symbols or dots giving one a sense of the bedrock outcrop control for the map. The data in the Bethel quadrangle was collected in the field seasons of 2011 and 2019 by Prof. J. Dykstra Eusden of Geology Department at Bates College with the help of these capable assistants: Riley Eusden (Bowdoin College '12); Thorn Merrill (Bates College '18), Kurt Niiler (Bates College '18), and Myles Felch (Maine Mineral and Gem Museum). James Brady did a M.S thesis (Brady, 1991; U. Maine Orono) that included the northern portion of the quadrangle and consisted of a set of very detailed bedrock and structural maps. These data, as well as conversations with him, were extremely helpful, and some of his data has been digitized and included on the new map. He is also a co-author of this map. To determine the absolute age of the rock types in the quadrangle two samples were radiometrically dated using U-Pb geochronology techniques on the mineral zircon. Dr. Justin Strauss of Dartmouth College's Earth Sciences Department performed the zircon mineral separations, Dr. Bill McClellend of the University of Iowa performed cathodoluminescence imaging of the zircons, and zircon dating was done at the LaserChron Center in the University of Arizona, Tucson. This publication has several parts, the most important of which is a geologic map showing the different rock types uniquely color coded and symbolized. There are two cross sections, along the lines labeled **A-A′** and **B-B′** on the map, which show the interpretation of the subsurface geology based on extending downward the data and interpretations from the Earth's surface. The **Explanation of Units** is a brief description of each rock type in the quadrangle with intrusive (once molten) rocks followed by stratified, or layered, mostly metasedimentary rocks next. These are listed by age with the oldest at the bottom of each section. The **Explanations of Lines** and **Symbols** serve to explain the significance of all of the artwork on the map. The photo gallery shows representative outcrop images of key units and boundaries observed in the field. The map was made and edited by the Maine Geological Survey.

GEOLOGIC OVERVIEW

Bedrock that underlies the western portion of the Bethel quadrangle is composed of stratified, or layered, rock of probable Silurian age (**Photos 3 – 10**) that was deposited as sediment on the seafloor in an ancient marine setting. The rocks were subsequently metamorphosed and deformed into folds by heat and pressure in the Devonian and Carboniferous Periods during the plate collisions of the Acadian, Neoacadian, and Alleghanian orogenies as the continents, from west to east, of Laurentia, Gander, Avalon, Meguma, and Gondwana successively collided to form the Appalachian Mountains (see **Geologic Time Scale** below).

Slightly less than half of the bedrock in the Bethel quadrangle, principally in the eastern part of the quadrangle, is composed of a single intrusive igneous rock or pluton, solidified from molten rock, called the Songo pluton. It is quartz diorite to granodiorite in composition with associated pinkish pegmatites (**Photo 2**). The Songo pluton is known to be Devonian based on a sample from the adjacent Bryant Pond quadrangle dated by Gibson and others (2017) at 364 ± 1.3 Ma. The Songo pluton was also deformed by both folding and shearing during the Neoacadian and Alleghanian orogenies.

There are also a few mappable regions of mostly two-mica granite and ubiquitous white pegmatites that were injected into the metamorphic rocks. There are also many of these that are too small to show on the map, especially the pegmatites. The smaller granitic plutons and pegmatites likely range in age from middle Devonian to Permian. In the adjacent Gilead quadrangle two different two-mica granite sills near Wheeler Mine were dated to be circa 350 Ma placing them, within error, on the Devonian-Carboniferous time boundary (Eusden and others, 2018). These granites extend into the southwestern corner of the Bethel quadrangle.

Most of the quadrangle experienced extreme metamorphic conditions turning the rocks into migmatite (rock that partially melted and solidified nearly in place). The migmatization likely occurred in the Late Devonian to Early Carboniferous time period. Four small regions exist that escaped migmatization and these are shown by a black solid or dashed line with hachures, isolated from the areas with abundant migmatite.

The map also shows a variety of folds that formed when the rocks were extremely ductile during the Devonian and Carboniferous plate collisions of the Acadian, Neoacadian, and Alleghanian orogenies, or mountain building events. There is one Acadian fold axis shown as a blue line with symbols on the map representing the earliest fold to form, called F_1 folds, and that only folds the metasedimentary rocks. Two other folds shown with dashed blue lines represent the younger Neoacadian F_2 folds that refolded the earlier F_1. These later F_2 folds deform both the migmatized metasedimentary rocks and the Songo pluton.

A late, brittle, Jurassic(?), normal(?) fault was also mapped along the southeast flank of Farwell Mountain. Outcrops of quartz that form a long, southwest- to northeast-striking silicified zone mark the fault (**Photos 1A** and **1B**). This fault likely formed during the rifting of Pangea and opening of the Atlantic Ocean.

Glacial deposits cover much of the bedrock and glacial erosional features can be seen on many of the outcrops. The reader is referred to the surficial geologic map of Thompson (2008) for a complete discussion of the glacial history that extends back to about 20,000 years ago.

STRATIFIED ROCKS

Mapping in the Bethel quadrangle revealed ten different metasedimentary units defining a stratigraphy that best correlates to the Silurian stratigraphy seen in the Rangeley, Maine, region (Moench and others, 1999), and more specifically the Rangeley, Perry Mountain, and Smalls Falls Formations. The stratigraphy in Bethel is poorly controlled by graded beds, which would typically allow one to establish the relative order of the units. Only a few graded beds from the original deposition as marine sediments were found in the region largely because the prevalent migmatite has obscured these primary sedimentary features. Lithologic correlation of units in Bethel to those of Rangeley, Maine, stratigraphy coupled with the new geochronology results, discussed below and as reported for the adjacent Gilead quadrangle (Eusden and others, 2018), support the conclusion that these rocks are Silurian. The presence of belts of moderately rusty and deeply rusty weathering schists and quartzites, non-rusty-weathering biotite and calc-silicate granofels, and ubiquitous pods, blocks, and lenses of calc-silicate rocks, represented by the units **Ssq**, **Ssqg**, **Ssg**, **Ssrc**, **Ssrcg**, **Ssqc**, and **Ssr**, are hallmarks of the Rangeley Formation in nearby New Hampshire (Eusden, 2010). The clean, light gray to white quartzites of the **Sqs** unit are typical of the Perry Mountain Formation, while the deeply rusty weathering schists of unit **Ssqr** are typical of the Smalls Falls Formation (Moench and others, 1999). We interpret the oldest rock in the stratigraphy to be unit **Ssr** found in a belt striking northeast to southwest across the northwest portion of the map. The youngest unit is **Ssqr** that can be found in both the northwest and southwest corners and also in the Farwell Mountain region in the center east part of the map. The stratigraphy is mapped in two regions: (1) a belt along the western edge of the quadrangle; and (2) the isolated Farwell Mountain block. The western section shows a mirror image pattern on either side of the oldest unit **Ssr**. We interpret this to be due to an early F_1 antiformal fold, through the middle of **Ssr**, that repeats the pattern. There is some graded bedding control in the northeastern part of the quadrangle and abundant reversals of graded bedding just to the north in the Puzzle Mountain quadrangle as mapped by Brady (1991) that support the placement of this early F_1 fold axial trace. The Farwell Mountain block sits isolated from the western section atop the Songo pluton and the units mapped within it correlate extremely well to those in the west. The Farwell Mountain block is folded into an antiformal syncline of F_2 age.

Compared to the most recent previous geologic map that included the Bethel region (Moench and others, 1999), the current bedrock geologic map shows no evidence at the surface of the Devonian Littleton or Silurian Madrid formations. The Littleton Formation formed the bulk of the previous map of Bethel while the Madrid Formation consisted only of small slivers. The absence of exposed Littleton and Madrid formations here agrees well with the recent map of the Gilead quadrangle immediately adjacent to the west (Eusden and others, 2018). Despite the lack of apparent surface exposures of these two formations, there is shown at depth in the core of the recumbent syncline on the cross sections, units of rock that are similar to the Madrid Formation (**Sgf**) and the Littleton Formation (**Dl/Dc**). These are inferred to be present based on the known stratigraphy, the structure, and correlations from adjacent New Hampshire and the Presidential Range (Eusden, 2010).

Comparisons to Brady's (1991) M.S thesis map show good agreement with his suggestion, termed Scheme 2, that the rocks in the Bethel quadrangle he named the Central and Southern Sequences are mostly Silurian and dominantly Rangeley Formation equivalents. Some differences between Brady's map and this map do exist. In the northeast border region of the map, along and adjacent to Stony Brook, the deeply rusty weathering schists and gray quartzites and schists that he mapped in his Central Sequence as the Smalls Falls Formation and Perry Mountain Formation respectively, we interpret as a rusty-weathering section and well-bedded section of the Rangeley Formation (units **Ssrc** and **Ssqc**, respectively). This interpretation is strengthened by on-strike connections to very similar rocks on Mount Will, Locke Mountain, and Ellingwood Mountain. This stratigraphic interpretation would also require the elimination of the pre-metamorphic Blueberry Mountain Fault shown by Brady (1991) on the north flank of Farwell Mountain and separating his Central and Southern Sequences. We saw no evidence for the fault, and on the Brady (1991) map it was shown in a region with very limited outcrop control. In summary, we suggest that the entire stratigraphy of the Bethel quadrangle is equivalent to Brady's (1991) Southern Sequence and we agree with his Scheme 2 stratigraphic correlation where the rocks are mostly Rangeley Formation equivalents.

The nature of the stratified rocks suggests several things regarding the paleo-environment of the marine depositional basin. Regions of evenly bedded layers record relatively uninterrupted deposition of layer upon layer in a marine basin over perhaps several millennia. In contrast, the presence of the blocks, pods, and lenses of bedded fragments of calc-silicate rocks within a finer grained matrix suggest that these units were formed by catastrophic sub-marine debris flows. The blocks were broken up, perhaps triggered by earthquakes in what was a seismically active basin, and then transported to deeper water to ultimately be embedded in a clay matrix. An alternative hypothesis we favor less for these blocks is that the process of migmatization disrupted them after deposition and during the metamorphism. The rusty- and non-rusty-weathering nature of the units records times when the basin of deposition was either deprived of oxygen or not. Oxygen-poor basins are considered anoxic and typically lead to the formation of the iron sulfide minerals pyrite and pyrrhotite in the sediments. When these minerals are exposed to the surface by erosion, they weather to become rusty brown schists. Non-rusty-weathering rocks record times when the basin had better oxygenation and circulation. These variations in ocean circulation and available oxygen were largely due to the construction and removal of sea floor barriers to circulation created during active plate collisions and related deposition of sediment barriers.

A sample was collected from unit **Ssrcg** for detrital zircon age determination (see **Table 1, Location B**). The maximum depositional age as shown on **Figures 1** and **2** is circa 430 Ma, placing the sedimentation in the Wenlock Epoch of the Silurian Period. This confirms the Silurian designation of the stratigraphy and agrees well with detrital zircon ages of 427-430 Ma for the Rangeley Formation at the type section done by Bradley and O'Sullivan (2016). However, it is worth noting that all these ages are somewhat younger than the fossil-based age of 440 Ma for the Rangeley Formation at the type locality near Blanchard Pond in Rangeley, Maine.

INTRUSIVE ROCKS

Three broad types of intrusive igneous rocks were found in the Bethel quadrangle: (1) the quartz diorite/granodiorite of the Songo pluton (**Ddg**) and associated pinkish pegmatite; (2) muscovite-biotite granite (**CDg** and **PDgm**); and (3) pegmatite (**PDgm** and **Pp**).

The oldest intrusive rock in the quadrangle, based upon cross-cutting relationships, is the Songo pluton (**Ddg**). It covers most of the eastern half of the quadrangle and is mapped as a single pluton with a maximum east-west width of about 10 kilometers (6 miles) and a north-south length of about 16 kilometers (10 miles). The pluton occupies the lower elevations of the quadrangle with limited outcrop as thick glacial till and outwash and post-glacial swamps often cover it. However, some key outcrops at Sparrowhawk Mountain, along the Androscoggin River near the confluence with the Sunday River, in Middle Intervale on the west flank of Farwell Mountain, and along Route 2 in Hanover, have helped delineate the western and northern boundary of the pluton. The eastern boundary of the Songo pluton is exposed in the adjacent Bryant Pond quadrangle. The pluton is likely a sub-horizontal sill 1 to 3 kilometers (0.6 to 1.9 miles) in thickness as inferred by gravity studies suggesting that within the sillimanite zone plutons become that shape and size (Hodge and others, 1982 and Nielson and others, 1976). We have speculated on the cross sections that the Songo pluton is thinner along **A-A′** and thicker along **B-B′** as one moves south toward the center of the pluton. The Songo extends under the metasedimentary sections of Farwell Mountain and the western portion of the quadrangle.

The Songo pluton is generally a coarse- to medium-grained quartz diorite to granodiorite. The mineralogy is mostly consistent with plagioclase, quartz, biotite, ± amphibole, ± potassium feldspar, ± sphene. Primary igneous layering composed of thin centimeter-scale leucocratic bands of biotite-absent quartz diorite/granodiorite is sporadically found. Irregular lenses and measurable veins of pink potassium feldspar pegmatite are found in many Songo outcrops and these are interpreted to be comagmatic with the Songo. Rare exposures of pink granite are found and have been interpreted as a phase of the Songo with more abundant potassium feldspar. There is also evidence of deformation in the Songo, as seen by shearing of igneous layering, the presence of biotite foliations, and broad-scale folding, all discussed further in the Deformation section below. The Songo pluton may correlate with the intrusive part of the Piscataquis Volcanic Arc (Bradley and Tucker, 2002), thought to be a subduction-related arc complex that formed during the Acadian Orogeny. The migmatite front, as defined in the Bethel and adjacent Gilead quadrangles, roughly parallels the western edge of the Songo pluton. This suggests that migmatization may in part be caused by the heat from the intruding Songo pluton.

A sample was collected from the Songo pluton for zircon crystallization age determination (see **Table 1, Location A**). **Figures 3** and **4** show that the crystallization age of the Songo Pluton in the Bethel quadrangle is 360.7 ± 2.2 Ma, placing the intrusion in the Late Devonian Period. This agrees well with Early Devonian crystallization ages for the Songo pluton reported by Gibson and others (2016) for the Bryant Pond quadrangle, and by Koteas for the North Waterford quadrangle.

There are six small two-mica (muscovite-biotite) granite plutons (units **CDg** and **PDgm**) in the Bethel quadrangle, four in the western metasedimentary section and two in the Farwell Mountain section. These appear as unfoliated, small, sill-like bodies. None appear to intrude the main body of the Songo pluton, but when the Songo contact is approached, two-mica granite bodies, all too small to map as separate units on the geologic map, are encountered. These granites are identical to granites of the Sebago pluton which have been dated to 288-297 ± 14 Ma, or within the Late Carboniferous to Permian period (Solar and Tomascak, 2016), as well as granites in the Presidential Range that have been dated to 363 Ma, or within the Late Devonian (Eusden, 2010), and to granites dated to 349.2 ± 2.1 and 355.3 ± 2.3 Ma (Carboniferous to Devonian in age) in the Gilead quadrangle (Eusden and others, 2018). Therefore, without geochronologic control, the muscovite-biotite granites are given a wide range of age from the Permian to Devonian, hence the symbol **PDgm**, or, where constrained in age, to the Carboniferous to Devonian, as the Gilead quadrangle, the symbol **CDg**. The muscovite-biotite granites cut the Songo along its contact, the migmatitic layering, and the late F_2 folds, and are in turn cut by pegmatites. The granites likely formed from melted continental crust and possibly also the melt derived from the migmatites.

The pegmatites, unit **Pp** and within unit **PDgm**, are one of the more common rocks in the Bethel quadrangle and most outcrops have at least some amount of pegmatite cutting through the older units. Nearly all these pegmatites are too small to show as separate units on the map. These pegmatites are younger than the pink pegmatites associated with the Songo pluton. The pegmatites cross-cut all other units and structures in the Bethel quadrangle except for a late brittle fault marked by a silicified zone. These pegmatites also likely formed from melted continental crust. The pegmatites in the Bethel quadrangle have not been dated but are likely as young as Permian or as old as Devonian based on the ages of similar pegmatites in New England determined by Bradley and others (2016). Nearly all these pegmatites are termed common pegmatites, meaning that they contain a simple mineralogy of quartz, feldspar, muscovite, ± biotite, rare black schorl tourmaline, and no multicolored tourmaline. Despite the abundance of gem-bearing pegmatite quarries in the Oxford Hills region, there are interestingly none in the Bethel quadrangle.

MIGMATITES

Migmatites are found throughout the metasedimentary rocks in the Bethel quadrangle. These partially melted rocks formed when high heat flow from other magmas, or perhaps the mantle, resulted in the partial melting of the stratified rocks. The lighter quartz- and feldspar-rich portions of the migmatites are thought to be the now-frozen melt fractions while the darker biotite-rich portions are the residual unmelted fractions. The process of migmatization happened when the rocks were very ductile and plastic and hot metamorphic fluids flowed through them, partially melting the rocks. This rendered the once-planar layering in the stratified rocks into a complex distorted and swirly orientation. The migmatites correlate well to the Sebago Migmatite-Granite Complex dated to 376 ± 14 Ma or the Late Devonian-Carboniferous period by Solar and Tomascak (2016) and Solar and others (2017). The four regions of non-migmatized metasedimentray rock have intact bedding and far less evidence of melting. It is likely that the heat from the intrusion of the Songo pluton contributed to migmatization. The two isolated non-migmatized sections in the center west of the map must have escaped migmatization due to the vagaries of metamorphic fluid flow through the rocks. The two non-migmatized sections on the north border of the map are part of a continuous migmatite front north of which the rocks show little melt and excellent preservation of primary layering. This boundary extends into the Gilead quadrangle to the west.

DEFORMATION

There are several phases of deformation that the rocks experienced during successive plate collisions. Eusden and others (2018) reported in the adjacent Gilead quadrangle the presence of rare pre-metamorphic faults that likely formed in an active tectonic setting probably just after deposition of the sedimentary rocks. Though no such features were found in the Bethel quadrangle, they could have easily been missed due to the extensive migmatization and lack of exposure.

As plate collisions commenced the first generation of folds formed, called F_1. These are recognized in the field by rare isoclinal folds, a strong axial planar S_1 schistosity that is most always parallel to bedding, and regions where the stratigraphy flips over and repeats itself by folding. The F_1 fold axial trace within unit **Ssr** is mostly based upon the apparent stratigraphic repetition around that unit as well as a few graded beds in the quadrangle and more graded beds in the adjacent Puzzle Mountain quadrangle (Brady, 1991). The units to the east of the F_1 axial trace are interpreted to be inverted, and those to the west are upright. The Farwell Mountain block is interpreted to be an extension of the inverted section. The F_1 folding pre-dated the migmatization.

The next folding event, F_2, is marked by common, centimeter- to meter-scale open folds, often with parasitic crenulations, sometimes a well-developed S_2 axial plane cleavage, and two regional folds shown as blue axial traces on the map determined by regional changes in the bedding and foliation. Steeply dipping axial planes and hinge lines plunging shallowly to the north or northeast characterize the geometry of the F_2 folds. π diagrams of bedding and S_1 foliation measurements in the western and Farwell Mountain sections of metasedimentary rocks show somewhat similar orientations for the F_2 hinge lines of 045°, 15° and 020°, 31°, respectively (**Figures 5** and **6**). Interestingly, biotite foliations in the Songo pluton show deformation and a π diagram of these data yield a 009°, 27° hinge line orientation which is also interpreted to be an F_2 fold (**Figure 7**). The regional F_2 fold axial trace in Farwell Mountain extends through the center of the metasedimentary units, where it would be classified as a synformal anticline, then extends to the south into the Songo pluton as a synform. Similarly, the second regional F_2 axial trace on the map in the metasedimentary rocks of Sparrowhawk Mountain, which would be classified as an antiformal syncline, extends north into the Songo pluton as an antiform. The foliation in the Songo likely formed after the development of the F_1 folds but before the development of F_2 folds. It is possible that the Songo foliations formed during the intrusion of the pluton as this fabric is parallel to compositional primary igneous layering when both are seen together. These fabrics were then subsequently folded by F_2 folds. In the adjacent Gilead quadrangle, Eusden and others (2018) reported that F_2 folds were cut by Songo equivalent diorites making the Songo younger than F_2. However, the outcrop control and foliation attitudes that constrain the timing of F_2 folds and the Songo intrusion are much better in the Bethel quadrangle, supporting the revised interpretation. Another possibility for the foliations in the Songo is that they represent discrete, variably oriented shears, internal to the pluton. However, the fold model is favored here due to the contiguous change in dip from the metasedimentary rocks into the Songo pluton.

Rare strike-slip shears of igneous compositional layering and biotite foliation in the Songo Pluton are seen. No consistent shear sense was observed as both left- and right-handed shears are apparent. These shears probably post-date the F_2 folding.

The silicified zone along the southeast flank of Farwell Mountain records the last deformation. These represent zones of silica-rich fluids flowing along a steeply northwest dipping fault that strikes northeast. It is likely a normal fault with the northwest side dropped down relative to the southeast side. The fault dies out to the southwest into the valley floor gravels of the Androscoggin River, so its extent is unknown. This fault is probably related to extension that occurred in the Jurassic during the rifting of Pangea.

SUMMARY

In summary, the major geologic events in Bethel quadrangle are: (1) Silurian deposition of the Rangeley Stratigraphy and, by inference to other regions to the west, Devonian deposition of the Littleton Formation; (2) Devonian Acadian Orogeny F_1 folding and the onset of regional metamorphism; (3) continued Devonian Acadian orogeny migmatization and Songo pluton intrusion and foliation; (4) Late Devonian Neoacadian F_2 folding: (5) Devonian to Carboniferous Neoacadian intrusion of two-mica granite plutons and some pegmatite; (6) Permian Alleghanian emplacement of the Sebago-type two-mica granite plutons and abundant pegmatites; and (7) Jurassic normal faulting during the rifting of Pangea.

GEOLOGIC TIME SCALE

Geologic Age	Absolute Age*
Cenozoic Era (**Cz**)	0-66
Mesozoic Era (**Mz**)	
Cretaceous Period (**K**)	66-145
Jurassic Period (**J**)	145-201
Triassic Period (**TR**)	201-252
Paleozoic Era (**Pz**)	
Permian Period (**P**)	252-299
Carboniferous Period (**C**)	299-359
Devonian Period (**D**)	359-419
Silurian Period (**S**)	419-444
Ordovician Period (**O**)	444-485
Cambrian Period (**Є**)	485-541
Precambrian time (**pЄ**)	Older than 541

* In millions of years before present (Ma). (Walker, J.D., Geissman, J.W., Bowring, S.A., and Babcock, L.E., compilers, 2012 Geologic Time Scale v. 4.0: Geological Society of America, doi: 10.1130/2012.CTS004R3C.)